Amino Acids (2015) 47:2265–2278
DOI 10.1007/s00726-015-2005-2

ORIGINAL ARTICLE

Hydration of amino acids: FTIR spectra and molecular dynamics studies

Aneta Panuszko[1] · Beata Adamczak[1] · Jacek Czub[1] · Emilia Gojło[1] · Janusz Stangret[1]

Received: 15 December 2014 / Accepted: 6 May 2015 / Published online: 23 May 2015

Abstract The hydration of selected amino acids, alanine, glycine, proline, valine, isoleucine and phenylalanine, has been studied in aqueous solutions by means of FTIR spectra of HDO isotopically diluted in H_2O. The difference spectra procedure and the chemometric method have been applied to remove the contribution of bulk water and thus to separate the spectra of solute-affected HDO. To support interpretation of obtained spectral results, molecular dynamics simulations of amino acids were performed. The structural-energetic characteristic of these solute-affected water molecules shows that, on average, water affected by amino acids forms stronger and shorter H-bonds than those in pure water. Differences in the influence of amino acids on water structure have been noticed. The effect of the hydrophobic side chain of an amino acid on the solvent interactions seems to be enhanced because of the specific cooperative coupling of water strong H-bond chain, connecting the carboxyl and amino groups, with the clathrate-like H-bond network surrounding the hydrocarbon side chain. The parameter derived from the spectral data, which corresponds to the contributions of the population of weak hydrogen bonds of water molecules which have been substituted by the stronger ones in the hydration sphere of amino acids, correlated well with the amino acid hydrophobicity indexes.

Keywords Amino acids · Hydration · Aqueous solutions · Hydrophobicity index · FTIR spectroscopy · Molecular dynamics

Introduction

Amino acids belong to a class of metabolites, called osmolytes, which are accumulated in living organisms as a protective system under unfavorable environmental conditions (Yancey et al. 1982). It is known that osmolytes increase protein stability against denaturation without significantly perturbing the functional activity of the proteins and other cellular components (Arakawa and Timasheff 1985; Arakawa et al. 2007; Taneja and Ahmad 1994; Wang and Bolen 1996, 1997). The stabilization of proteins by amino acids is manifested in the increased melting temperature of the proteins at both neutral and lower pH values (Anjum et al. 2000; Jamal et al. 2009; Taneja and Ahmad 1994). It has been observed that various amino acids have different effects on protein stability in terms of the melting temperature (Arakawa and Timasheff 1985; Shiraki et al. 2002; Taneja and Ahmad 1994).

Despite significant progress in understanding of the effect of presence an osmolyte on protein stability, the precise mechanism of stabilization is still not clear. There are several theories proposed to explain this effect. One of these theories assumes that osmolytes are preferentially excluded from the protein surface which is equivalent to preferential hydration of the proteins (Arakawa and Timasheff 1985; Bolen and Baskakov 2001; Liu and Bolen 1995; Timasheff 2002; Wang and Bolen 1997). As a

Handling Editor: J. Dai.

Electronic supplementary material The online version of this article (doi:10.1007/s00726-015-2005-2) contains supplementary material, which is available to authorized users.

✉ Aneta Panuszko
aneta.panuszko@pg.gda.pl

[1] Department of Physical Chemistry, Chemical Faculty, Gdańsk University of Technology, Narutowicza 11/12, 80-233 Gdańsk, Poland

consequence, it is also stated that osmolytes do not interact with proteins directly, but rather through the surrounding water of modifying properties (Bennion and Daggett 2004; Bruździak et al. 2013; Daggett 2006; Panuszko et al. 2009; Soper et al. 2003). Thus, to understand the effect of amino acids on protein stability it is important to understand their influence on the water structure and interactions between water molecules. Based on the concept that osmolytes stabilize proteins by causing the modification of water structure and due to the fact that various amino acids have different effects on the stability of proteins, it is expected that their influence on the structure of water will be also different, contrary to the previous findings in solution at neutral pH (Ide et al. 1997).

Aqueous amino acid solutions were extensively studied experimentally by IR spectroscopy (Hecht et al. 1993; Hernandez et al. 2009; Kumar et al. 2005; Olsztynska et al. 2001; Panuszko et al. 2011), NMR spectroscopy (Ide et al. 1997), Raman spectroscopy (Balabin 2010; Ide et al. 1997; Kumar et al. 2005; Zhu et al. 2011), THz spectroscopy (Niehues et al. 2011; Sun et al. 2014), neutron diffraction (McLain et al. 2007; Troitzsch et al. 2007), ultrasonic measurements (Burakowski and Gliński 2010), and theoretically by molecular dynamics methods (Campo 2006; Pacios 2001; Shirts and Pande 2005; Troitzsch et al. 2007) and by ab initio calculations (Chaudhari et al. 2004; Hernandez et al. 2009; Michaux et al. 2009; Mullin and Gordon 2009; Panuszko et al. 2011). Among these works, excluding our study on the hydration of glycine and its methyl derivatives (Panuszko et al. 2011), only two can be directly related to the results obtained by the method used by us. Ide et al. (1997) examined aqueous solutions of amino acids by Raman spectroscopy, by analysis of the intensity of H_2O stretching vibration band corresponding to an in-phase collective vibration of OH oscillators that are connected by hydrogen bonds. The authors concluded that at neutral pH various amino acids did not differ from one another significantly. They detected difference only after lowering or also raising pH of solutions. Thus only at acidic or basic conditions did the authors observe that degree of hydrogen bonding between water molecules is affected by side chains of amino acids. At this point we would like to draw attention that the so-called the collective OH band is not the only type of water OH vibration band. Thus collective bond is not representative for the whole population of water hydrogen bonding and then the presented method of analysis cannot give an adequate characteristic of solute influence in this respect. The paper of Hecht et al. (1993) presented difference infrared spectra between zwitterionic amino acid aqueous solutions and of pure H_2O at the 3800–2600 cm^{-1} region. Spectra differ depending on the amino acids. However, the differences obtained are of poor quality. Water OH bands in difference spectra obtained by authors indicate an overall increase in the degree of hydrogen bonding of water. Corresponding absorption growth has been approximated by one Gaussian component band with band position differing between 3437 and 3383 cm^{-1} in dependence of amino acid. However, we have established that a difference spectrum of H_2O in aqueous solutions, obtained in such a way to extract the solute-affected water spectrum, consists of at least four components (Śmiechowski and Stangret 2007, 2008; Stangret and Gampe 2005). Each of component bands corresponds to the different state of water H-bonds. Generally, results presented by the both discussed papers give definite oversimplified image of the state of water H-bonds in aqueous solution.

We specialize in gaining subtle information about the energetic and structural state of water molecules hydrating different solutes on the basis of vibrational spectra of water in solution (Śmiechowski and Stangret 2010). Vibrational spectroscopy is an ideally suited method for investigation of solute hydration. The time scale of response of vibrational spectroscopy, ~10^{-14} s, is in the range of water stretching vibrations, allows registering even relatively short-lived species formed by water molecules influenced by a solute. Vibrations of semi-heavy water (HDO), isotopically diluted in H_2O, have been used as a sensitive probe of local molecular surroundings and thus of solute hydration. HDO spectra are free of interpretive and experimental difficulties connected with H_2O spectra. The OD vibration is decoupled from all the other OH vibrations in the system and the local structure and dynamics around the OD vibration can be studied in the absence of any complication arising from molecular couplings.

To receive information about the structure and interactions inside the hydration sphere, the contribution of bulk water to the spectrum should be removed as to obtain the solute-affected spectrum. This has been done applying the quantitative version of the difference spectra method developed in our laboratory. More details on this and related topics can be found in the review (Śmiechowski and Stangret 2010).

The goal of our previous work was to characterize the state of water molecules hydrating the basic hydrophilic centers of glycine, i.e., the carboxyl and the amino group (Panuszko et al. 2011). It was preceded by studies of carboxylate anions hydration (Gojlo et al. 2009) as well as of the amino group (Panuszko et al. 2008) and also protonated amino group (Gojlo et al. 2005) hydration.

In this work, we used FTIR spectroscopy to investigate the hydration properties of selected amino acids with nonpolar side chain: alanine (Ala), glycine (Gly), proline (Pro), valine (Val), isoleucine (Ile) and phenylalanine (Phe) in water solution. On the basis of the band shapes of solute-affected HDO spectra, the energetic state and organization of affected water molecules in the presence of solute

were determined. The obtained spectral results were compared and discussed with the results of molecular dynamics simulations.

Experimental section

Chemicals and solutions

Alanine (Ala, 99 %, Aldrich), glycine (Gly, 99 %, Sigma), proline (Pro, 99 %, Aldrich), valine (Val, 99 %, Aldrich), isoleucine (Ile, 99 %, Aldrich) and phenylalanine (Phe, 99 %, Aldrich) were used without further purification.

Sample and reference solutions for FTIR measurements of HDO spectra have been prepared as described in the Supplementary Material. All solution densities were measured using an Anton Paar DMA 5000 densitometer at 25.000 ± 0.001 °C.

FTIR spectra of HDO measurements

FTIR spectra of aqueous solutions of amino acids were recorded on Nicolet 8700 spectrometer (Thermo Electron Co.) with a resolution of 4 cm^{-1}; 128 scans for each spectrum were made. The spectrometer was purged with dry nitrogen to eliminate the influence of water vapor and carbon dioxide on spectra shape. All the FTIR measurements were carried out using a liquid cell (model A145, Bruker Optics) with CaF_2 windows separated by Teflon spacers. The path length was 0.0289 mm and was precisely determined interferometrically. The temperature of measurements were kept at 25.0 ± 0.1 °C and monitored using electronic thermometer equipped with thermocouples placed in the sample cell.

The series of Ala, Gly and Pro solutions were in the range of molality (m) between 0 and 1 mol kg^{-1} (in ca. 0.2 mol kg^{-1} steps). For Ile and Phe solutions molalities were in the range between 0 and 0.14 mol kg^{-1} (in ca. 0.01 mol kg^{-1} steps), and between 0 and 0.4 mol kg^{-1} for Val (in ca. 0.1 mol kg^{-1} steps). Different concentration ranges result from the solubility of amino acids in water. In the case of each amino acid the dependence of molar absorption coefficient vs. molality (calculated at each wavenumber) has been approximated with a linear function ($R^2 > 0.9998$).

Analysis of spectral data

All spectra have been handled and analyzed using the commercial PC software: OMNIC (Thermo Electron Corporation), GRAMS/32 (Galactic Industries Corporation, Salem, NH) and RAZOR (Spectrum Square Associates, Inc., Ithaca, NY) run under GRAMS/32.

The difference spectra method has been applied to extraction the solute-affected HDO spectrum on the basis of spectra series measured for different molalities of aqueous solutions and the bulk HDO spectrum (Stangret 1988; Stangret and Gampe 1999). The method is based on the assumption that it is possible to divide water in solution into two additive contributions: the bulk water and the solute-affected water. These contributions correspond to the spectrum of bulk water identical to the pure water spectrum, ε_a, and the solute-affected water spectrum, ε_b, respectively.

The basis for isolation of the solute-affected water spectrum, extrapolated to the infinite dilution is shown in Eq. (1):

$$\varepsilon_a = \frac{1}{NM}\left(\frac{\partial \varepsilon}{\partial m}\right)_{m=0} + \varepsilon_b, \tag{1}$$

where N parameter is the "affected number", equal to the number of moles of water affected by one mole of solute, M is the mean (4 % D_2O in H_2O in the case of HDO spectra) molar mass of water (kg mol^{-1}), and m denotes the molality of the solution (mol kg^{-1}). The derivative, $\partial\varepsilon/\partial m$, in the infinite dilution limit, is received by an approximation of the molar absorption coefficient value as a function of molality at each wavenumber using linear or quadratic regression.

The detailed procedure method of spectral data analysis toward extraction of the solute-affected water spectrum was previously described (Bruździak et al. 2010, 2012; Śmiechowski and Stangret 2010; Stangret 1988). This method is used extensively in our laboratory inter alia to study of the hydration of aqueous solutions of molecules of biological importance such as osmolytes and proteins (Bruździak et al. 2013; Panuszko et al. 2009, 2011, 2012). The effectiveness of this method has been confirmed by molecular dynamics simulations (Panuszko et al. 2008, 2009, 2012) as well as by chemometric analysis of HDO spectra in aqueous solutions (Bruździak et al. 2010).

Molecular dynamics simulations

The simulated systems consisted of a single amino acid molecule (Gly, Ala, Pro, Val, Ile or Phe) in the zwitterionic form, confined in a cubic box of water molecules with a minimal distance between the solute and the box edge of 1.2 nm. Molecular dynamics (MD) simulation was performed using the GROMACS package (Hess et al. 2008) and the GROMOS53a6 force field (Oostenbrink et al. 2005) for amino acid molecules. To capture possible subtle differences in the structural and dynamic properties of amino acid hydration shells, we used a flexible water model with anharmonic bond potentials (Praprotnik et al. 2004).

Molecular dynamics simulations were carried out in the NPT ensemble at 300 K and at 1 bar using the Berendsen weak coupling method (Berendsen et al. 1984) to control both the temperature and pressure, with a relaxation time of 0.1 and 1 ps, respectively. Periodic boundary conditions were applied and the Particle Mesh Ewald method (Darden et al. 1993) with a real-space cutoff of 1 nm and a grid spacing of 0.1 nm was used to evaluate electrostatic forces. The systems were simulated for 100 ns using a time step of 0.5 fs which allowed for full intramolecular flexibility of the solvent molecules. A geometric criterion for the hydrogen bond existence was used for calculation of the intermolecular distance R_{OO} distribution (Kumar et al. 2007). According to this criterion a hydrogen bond is present when the distance between the donor and the acceptor is less than $r_0 - \alpha\theta^2$, where θ is the acceptor–donor-hydrogen angle and the parameters r_0 and α were set to 0.32 nm and 4×10^{-5} nm deg^{-2}, respectively.

Results and discussion

To understand better the results obtained in this paper for amino acid hydration, previously established facts and observation have to be taken into account.

Our results obtained from IR studies, and supported by MD and DFT calculations, for hydration of mixed hydrophobic-hydrophilic type solutes can be explained most coherently assuming "clathrate structure" (Head-Gordon 1995)—clathrate-like type hydration. This clathrate water cage is perturbed by H-bonds formed with the solute hydrophilic groups. It is only the quantitative issue in which case the perturbed or non-perturbed structure predominates (see distinction between TMAO and urea hydration; Panuszko et al. 2009). Sometimes, this evokes problems of the semantic nature. Water molecules from the first hydration sphere are on average parallel to the surface of the solute, which strongly suggests clathrate-like type hydration. Practically no orientation and energetic effects are observed outside the first hydration sphere.

Naturally, water–water H-bond network is perturbed to the least extent in the surrounding of non-polar part of the solute. For the hydration sphere of a hydrophobic solute which does not possess any hydrophilic groups, the general observation is compatible with the results obtained from the neutron diffraction method (Finney and Soper 1994; Finney 1996; Turner and Soper 1994)—the difference between the hydration sphere and the bulk water is very subtle. IR spectroscopy reveals that these differences comprise different distribution of water H-bonds and corresponding intermolecular distances: the energetic state of hydration water H-bonds and O···O distances are on average the same as for bulk water, but at the same time the population of H-bonds around the solute is greater, though these hydrogen bonds are disturbed, being less linear (Pieniazek and Stangret 2005; Stangret and Gampe 1999). Water in the hydration shell appears to have a weakly bonded ice-like structure, in accordance with the general view presented recently by Galamba (2013) on the basis of MD studies. Therefore, the applied method enables us to see the structure and energetic state of some distinguished water molecules, which reflect the effect of many more molecules surrounding the solute. This way, solute-affected water spectra represent the water in a "condensed" manner. This, along with the short time scale of vibrational spectroscopy, is the main cause of the high sensitivity of the method to differentiate various states of solvent molecules in the solution. Therefore, it is not surprising that other direct experimental methods, like neutron diffraction (Finney and Soper 1994; Finney 1996; Turner and Soper 1994) cannot show significant difference between water in the hydration sphere of hydrophobic solute and in the bulk phase, even for solution of high concentration.

The solute-affected water spectra we have obtained in hydration studies correspond to the N parameter, called as water-affected number, which should not be confused with "hydration number", obtained from diffraction experiments or MD simulations. N is close to the "hydration number" only when the solute-affected water band differs sufficiently from the bulk water band, either in position or in band-shape. Otherwise, affected number is lower than the "hydration number". This is especially the case for water molecules from the hydration sphere of hydrophobic molecules. For instance, N values obtained for $Bu_4N^+X^-$ (X = Br, Cl, and F) equal 7.4 ± 0.7, 8.1 ± 0.8 and 9.7 ± 1.0, respectively (the greatest contribution in N value falls to the anion; Stangret and Gampe 1999). On the other hand, the $Bu_4N^+X^-$ 32.8H_2O ideal formula is known for solid clathrate hydrates (McMullan and Jeffrey 1959; McMullan et al. 1963) and a "hydration number" of 46 has been published for the Bu_4N^+ cation in solution (Eriksson et al. 1988).

It is not possible to isolate the solute-affected water component band corresponding to the hydrophobic hydration in the case of a solute of the mixed hydrophobic-hydrophilic type because the effects of the hydrophobic and the hydrophilic hydration are not additive. We have observed how hydrophobic effect of the alkyl side chain is influenced by polarizing power exerted on the water molecules by the hydrophilic group of 2-butylamine (Gojlo et al. 2005). This effect is cooperatively transmitted to the interactions inside the clathrate-like water "cage" around the alkyl group, strengthening it. The interaction with the solute donor group does not, however, perturb significantly the already existing hydrophobic "cage" around non-polar part of the solute. This observation seems to be of general nature and

was confirmed for numerous solutes differing in electron-donor ability (Gojlo et al. 2007). Such mixed type of hydration results also in increasing the water-affected number (N), as water molecules taking part in hydration of the hydrophobic part of the solute become a source of vibration band which differs more in the band-shape and position in respect to the case of "pure" type of hydrophobic hydration, which in turn give vibration band very similar to the ones of the bulk water.

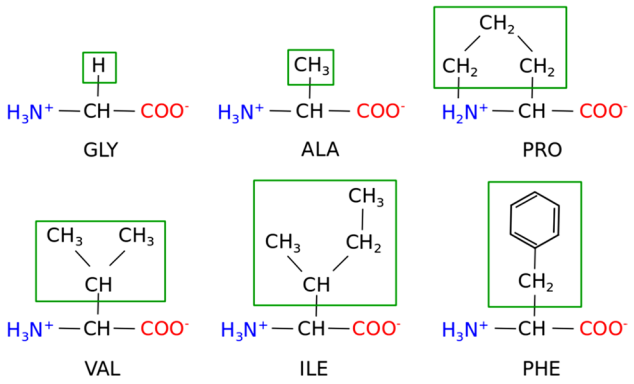

Fig. 1 The structures of amino acids in the zwitterion form: glycine (Gly), alanine (Ala), proline (Pro), valine (Val), isoleucine (Ile) and phenylalanine (Phe)

Solute-affected HDO spectra

Figure 1 shows the structures of analyzed amino acids in the zwitterionic form. Amino acid-affected water spectra include not only the absorption of HDO but also absorption contribution of isotopically substituted amine groups (N-D stretching vibrations), which has been removed using the procedure described in "Supplementary Material".

Figure 2 presents the solute-affected HDO spectra for amino acids (without the contribution of ND vibrations) decomposed into physically meaningful bands. The procedure of decomposition of the solute-affected water spectra has been described in "Supplementary Material". The number of component bands results from adequate fitting the band shape of solute-affected HDO spectra with a minimal number of analytical bands while remaining consistent with previous findings on the hydration of glycine and its methyl derivatives (Panuszko et al. 2011), which in turn are based on findings related to the hydration of carboxylate anions (Gojlo et al. 2009) and amides (Panuszko et al. 2008). Amino acid-affected HDO spectra are characterized

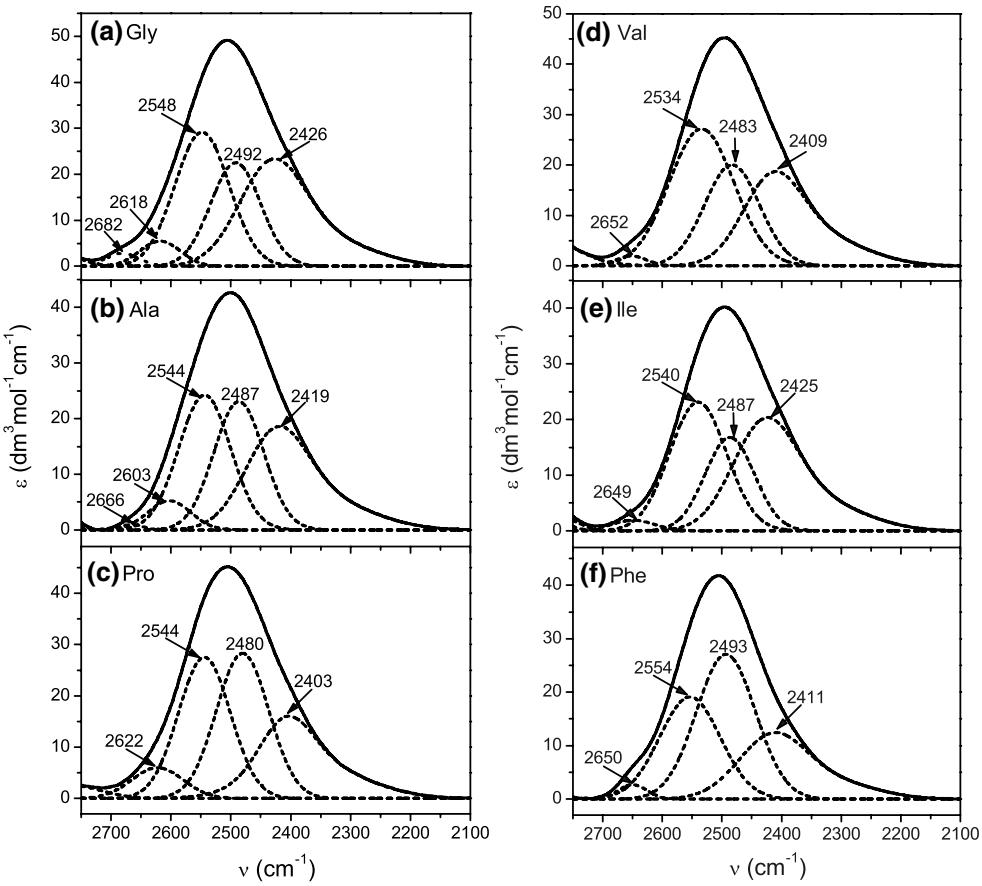

Fig. 2 Decomposition of affected spectra in the OD stretching region of HDO for **a** Gly, **b** Ala, **c** Pro, **d** Val, **e** Ile and **f** Phe into component bands. *Solid black line* indicates original affected spectrum; *dotted black line* indicates sum of the component bands (covered by the *solid line* of the original spectrum); *dashed black line* indicates OD component bands

among others by the presence of two component bands at 2544 ± 10 and 2487 ± 7 cm^{-1}, which are related to HDO molecules interacting with the oxygen atoms of the carboxyl group. The positions of these bands are consistent with the results of the spectral analysis of water affected by glycine and its methyl derivatives (Panuszko et al. 2011) and the carboxylate anions (Gojlo et al. 2009). Water molecules involved in proton transfer within the amino acid molecule, linking the carboxylic and amino group, give rise to the band at 2416 ± 13 cm^{-1}, whereas HDO, weakly interacting with the hydrogen atom of amine group, shows the band at 2614 ± 11 cm^{-1}. It should be noted that the urea-affected HDO spectrum shows similar small component band at 2631 cm^{-1}, which is due to a water molecule weakly interacting with the hydrogen atom of the amino group (Panuszko et al. 2008, 2009). The above-mentioned assignments of component bands follow from previous findings (Gojlo et al. 2009; Panuszko et al. 2008, 2011). Disappearance of the component band at 2614 ± 11 cm^{-1} in the case of Ile, Val and Phe can be explained assuming that water molecules which are normally forming weak H-bond with the amine group (and normally revealing the band at ca. 2611 cm^{-1}) (Panuszko et al. 2011) are now incorporated into the pseudo-clathrate water structure surrounding the side chain of amino acid. It should be remembered that water molecules from the hydration sphere of the hydrophobic solutes resemble the bulk water (Pieniazek and Stangret 2005; Stangret and Gampe 1999, 2005). The component band at 2650 ± 2 cm^{-1} arises most probably from vibrations of these water molecules of the pseudo-clathrate surrounding the hydrophobic side chain, which simultaneously experience the OD contact with the α-proton of the amino acid. High-wavenumber component band present in HDO spectrum affected by Ala and Gly (Fig. 2a, b), at 2674 ± 8 cm^{-1} is derived from not completely compensated own vibrations of these solutes. It may be suggested that clathrate-like water structure surrounding the side chain can have even reinforced structure, relative to the other hydrophobic groups or solutes, due to the specific cooperative coupling of water H-bonds chain connecting the carboxyl and amino group of the amino acid molecule (Panuszko et al. 2011, see Fig. 5 in this reference). This opinion will be justified in subsequent discussion of obtained results.

Figure 3a shows the solute-affected HDO spectra from Fig. 2, together with the bulk spectrum, scaled to the same maximum absorption value for better comparison. Band shapes of these spectra were compared and additionally transformed into the oxygen–oxygen distance distribution function $P(R_{OO})$ of the water molecules (Fig. 3b), according to Eq. (2):

$$R_{OO}/\text{Å} = [16.01 - \ln(2727 - \nu_{OD}/\ \text{cm}^{-1})]/3.73 \qquad (2)$$

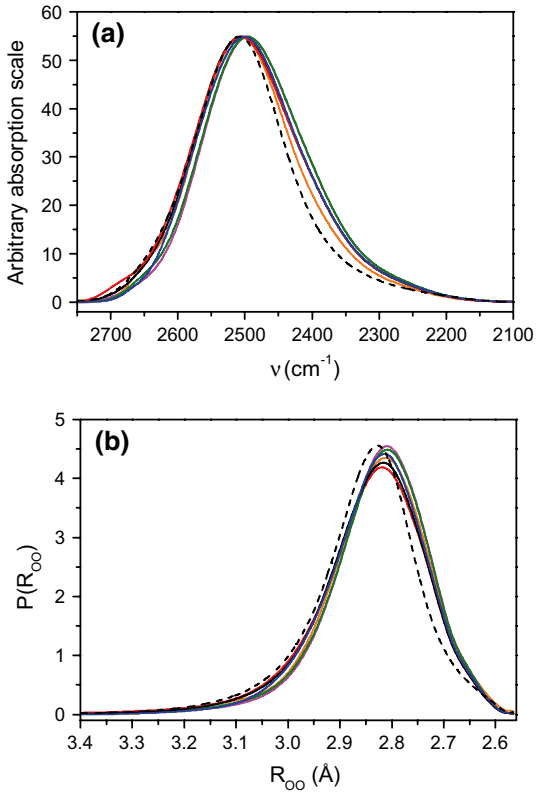

Fig. 3 **a** Solute-affected HDO spectra in the OD stretching region for Gly (*red*), Ala (*blue*), Pro (*black*), Val (*green*), Ile (*pink*) and Phe (*orange*) together with the bulk HDO spectrum (*black*, *dashed*). The spectra have been scaled to the same maximum absorption value for better comparison. **b** Interatomic oxygen–oxygen distance distributions function derived from the HDO spectra affected by Gly (*red*), Ala (*blue*), Pro (*black*), Val (*green*), Ile (*pink*) and Phe (*orange*), along with the bulk HDO (*black*, *dashed*) distance distribution curve (color figure online)

The equation linking ν_{OD} to R_{OO} was established on the basis of vibrational spectra and neutron diffraction measurements on solid hydrates (Berglund et al. 1978). It has been verified many times that this correlation is working well for aqueous solution (Bratos et al. 2009). The band parameters for all studied amino acid-affected HDO bands, together with the bulk HDO band, are shown in Table 1, along with intermolecular oxygen–oxygen distances, R_{OO}.

On the basis of the Badger–Bauer rule (Badger and Bauer 1937), which states that water hydrogen-bond energy changes linearly with the shift in OH (OD) band position, it is possible to define the energetic state of water molecules in hydration spheres of selected amino acids. The value of the maximum of absorption band position (ν^o) refers to the most probable hydrogen-bond energy, and the value of the gravity center band position (ν^g) corresponds to the mean energy of water hydrogen bonds. Accordingly, we recognized the most probable (R^o_{OO}) and

Table 1 Band parameters of HDO affected by amino acids, and for the bulk water bands as well as the respective intermolecular oxygen–oxygen distances

Solute	N^{a}	$\nu_{OD}^{o\ b}$	$\nu_{OD}^{g\ c}$	$Fwhh^{d}$	I^{e}	$R_{OO}^{o\ f}$	$R_{OO}^{g\ g}$
Bulk		2509 ± 2	2505 ± 2	162 ± 4	10,046	2.823 ± 0.003	2.844 ± 0.003
Gly	11.0 ± 0.5	2505 ± 2	2495 ± 2	185 ± 4	9986	2.821 ± 0.003	2.831 ± 0.003
Ala	11.9 ± 0.5	2500 ± 2	2490 ± 2	183 ± 4	8530	2.819 ± 0.003	2.827 ± 0.003
Pro	11.2 ± 0.5	2505 ± 2	2494 ± 2	185 ± 4	9114	2.819 ± 0.003	2.829 ± 0.003
Val	8.9 ± 0.5	2496 ± 2	2484 ± 2	184 ± 4	9077	2.809 ± 0.003	2.819 ± 0.003
Ile	10.2 ± 0.5	2496 ± 2	2482 ± 2	178 ± 4	7929	2.809 ± 0.003	2.819 ± 0.003
Phe	16.0 ± 0.5	2502 ± 2	2488 ± 2	184 ± 4	6738	2.809 ± 0.003	2.824 ± 0.003

R_{OO} errors have been estimated on the basis of the HDO bands position errors

[a] Affected number (see text)

[b] Band position at maximum (cm^{-1})

[c] Band position at gravity center (cm^{-1})

[d] Full width at half-height (cm^{-1})

[e] Integrated intensity ($dm^3\ mol^{-1}\ cm^{-1}$)

[f] The most probable O···O distance (Å)

[g] The mean O···O distance (Å)

the mean (R_{OO}^{g}) intermolecular oxygen–oxygen distance of water. In the case of water "structure-making" solutes the value of the center of gravity of OD band is shifted towards lower wavenumbers with respect to the corresponding position for pure water. It is accompanied by the shortening of oxygen–oxygen intermolecular distance. For the "structure-breaking" solutes it is shifted towards higher wavenumbers with increasing of the oxygen–oxygen intermolecular distance.

The most probable distance (R_{OO}^{o}) and the mean distance (R_{OO}^{g}) for the studied amino acids are shifted toward shorter values with respect to the corresponding ones for pure water (Table 1). From Table 1 it follows that the mean energy of water hydrogen bonds in the amino acid hydration sphere decrease in the following order: Ile > Val > Phe > Ala > Pro > Gly > bulk water. Thereby, Ile appears as the most water "structure-making" solute among the studied amino acids.

To provide greater insight into the difference in intermolecular distances, $\Delta P(R_{OO})$ has been calculated, the result of subtraction of the distribution function for amino acids-affected water, $P^{a}(R_{OO})$, and for bulk water, $P^{b}(R_{OO})$ shown in Fig. 4a for each studied amino acid. On the basis of the difference in intermolecular distance distribution (Fig. 4a) it may be seen that population of weak hydrogen bonds of water around amino acids decreases. Concurrently, the probability of the occurrence of short hydrogen bonds in water affected by amino acids increases. All selected amino acids enhance in this respect water structure in their surroundings.

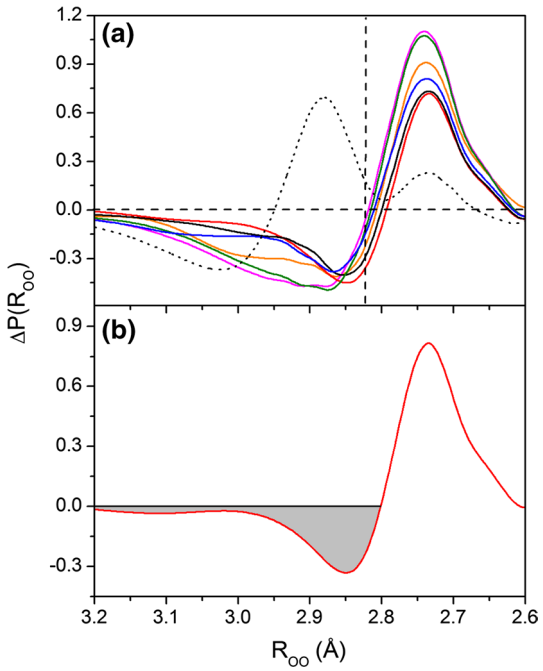

Fig. 4 **a** Differences between interatomic oxygen–oxygen distance distribution function of affected water, $P^{a}(R_{OO})$ and the bulk water, $P^{b}(R_{OO})$, calculated as $\Delta P(R_{OO}) = P^{a}(R_{OO}) - P^{b}(R_{OO})$: Gly (*red*), Ala (*blue*), Pro (*black*), Val (*green*), Ile (*pink*), Phe (*orange*) and tetrabutylammonium cation (*dotted black*) (Panuszko et al. 2008; Stangret and Gampe 1999). The *vertical dashed line shows* the position of the most probable distance for bulk water. **b** Illustration of the method of calculating the area corresponding to the population of weak hydrogen bonds of water molecules, which have been replaced by the stronger ones in the hydration sphere of the solutes (color figure online)

Table 2 The contributions of vanishing weak hydrogen bond population in the hydration shell of solutes, solvent-accessible surface of solutes and values for selected scales of hydrophobicity of amino acids

Solute	α^{a}	$\Delta\alpha^{c}$	β^{d}	$\Delta\alpha/\beta \times 10^{-4e}$	1[f]	2[f]	3[f]	4[f]
Gly	0.053	–	–	–	−0.4	0	−0.74	−0.57
Ala	0.071	0.018	24.14	7.48	1.8	0.2	−0.11	0.17
Pro	0.062	0.009	70.48	1.34	−1.6	−2.2	−2.23	−0.21
Val	0.101	0.048	75.91	6.35	4.2	4.7	0.31	1.21
Ile	0.107	0.054	101.64	5.30	4.5	4.8	0.60	2.06
Phe	0.085	0.032	142.29	2.23	2.8	4.4	0.32	1.29
Bu_4N^+	0.061[b]	–	582.35	1.05				

[a] The parameter which reflects the contribution of vanishing weak hydrogen bonds of water molecules. The α parameter was calculated as the area (see Fig. 4b and text)

[b] The value for tetrabutylammonium cation, calculated for the difference in the intermolecular distance distribution function $\Delta P(R_{OO})$ shown by Panuszko et al. (2008) and obtained on the basis of the results presented by Stangret and Gampe (1999)

[c] The α parameter for the amino acid relative to glycine ($\alpha_a - \alpha_{gly}$), determining the contribution of vanishing weak hydrogen bonds of water molecules around the amino acid side chain

[d] The solvent-accessible surface for the amino acid side chain and for Bu_4N^+ ion (Å^2)

[e] The contribution of vanishing population of weak hydrogen bonds of water molecules per unit surface of the side chain ($\Delta\alpha/\beta$ for amino acids and α/β for Bu_4N^+ ion) (Å^{-2})

[f] Hydrophobicity values taken from (1) Kyte and Doolittle (1982), (2) Cornette et al. (1987), (3) Hessa et al. (2005) and (4) Cid et al. (1992)

Contributions of the population of weak hydrogen bonds of water molecules

It is possible to quantitatively characterize the population of hydrogen bonds formed by water molecules present around the amino acids. On the basis of the difference in the intermolecular distance distribution (Fig. 4a), the vanishing population of weak hydrogen bonds of water molecules was calculated as the area, α (as shown in Fig. 4b). These values correspond to the contributions of the population of weak hydrogen bonds of bulk water which have been substituted by the stronger ones in the hydration sphere of amino acids. They are shown in Table 2. It can be seen that the parameter α decreases in the following order: Ile > Val > Phe > Ala > Pro > Gly. Decrease of weak hydrogen bonds of water molecules in the hydration sphere is characteristic for hydrophobic solutes—it is a sign of hydrophobic hydration. This effect can also be observed in the case of tetrabutylammonium cation (Fig. 4a), studied previously in our laboratory as a model for hydrophobic hydration (Stangret and Gampe 1999). It is possible to compare the results obtained for tetrabutylammonium cation and amino acids, namely determine the influence of the side chain on surrounding water molecules. It is noted that the α parameter for the amino acids reflects the contribution of vanishing weak hydrogen bonds of water molecules surrounding the amino acid molecule: around side chain, as well as those water molecules involved in hydrogen bonds formation with the hydrophilic groups of amino acids. Therefore, we used the glycine molecule as a model which takes into account interactions of water molecules with the amino and carboxyl group, occurring in the case of all amino acids. The contribution of vanishing weak hydrogen bonds of water molecules around amino acids side chain, $\Delta\alpha$, has been obtained by subtracting the value of parameter α corresponding to glycine from the value of the parameter α for each other amino acids. Then, we calculated the obtained $\Delta\alpha$ value per unit solvent-accessible surface of side chain. The solvent-accessible surfaces of amino acid side chain and of Bu_4N^+ ion, β , have been calculated by the grid method described by Bodor et al. (1989) using the atomic radii (Gavezzotti 1983) implemented in HyperChem 8.0.3 software. The applied procedure allowed calculation of the vanishing population of weak hydrogen bonds of water molecules per unit surface of the side chain, $\Delta\alpha/\beta$. All the respective data used for calculations are included in Table 2. These results show that the vanishing population of weak hydrogen bonds of water molecules (which have been substituted by the stronger ones in the hydration sphere of amino acids) per unit surface of the side chain decreases in the following order: Ala > Val > Ile > Phe > Pro > Bu_4N^+. The same order we obtained by converting the contribution of vanishing weak hydrogen bonds of water molecules per unit volume and solvent accessible volume of the side chain. It is worth noting that the smallest side chain (methyl group in alanine), has the greatest ability to organize a surrounding water molecules. A smaller contributions of vanishing weak hydrogen bonds of water molecules around the tetrabutylammonium cation means that interactions between water molecules around the side chains of the amino acid are numerous and stronger than around the hydrophobic molecule such as Bu_4N^+. This

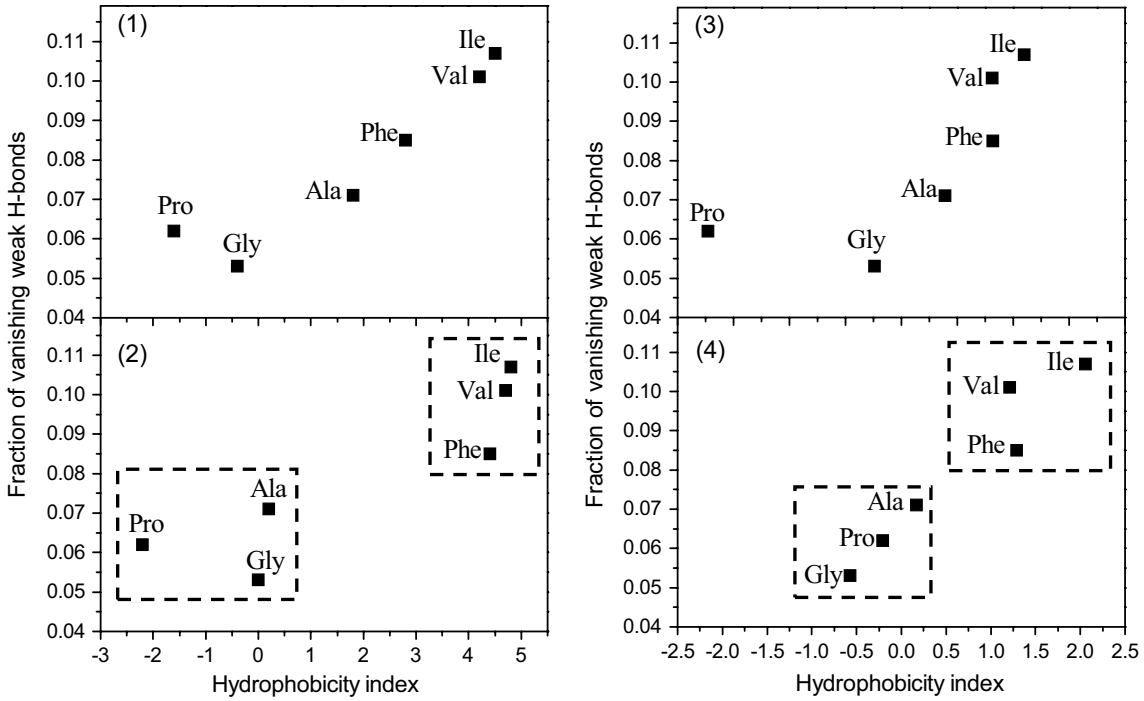

Fig. 5 Correlation between the contributions of vanishing weak hydrogen bond population (see Fig. 4b) and the amino acid hydrophobicity values: *1* Kyte and Doolittle (1982); *2* Cornette et al. (1987); *3* Hessa et al. (2005) and *4* Cid et al. (1992). All hydrophobicity indexes and area values are summarized in Table 2

confirms the earlier statement that the hydrophobic hydration of the hydrophobic side chain of an amino acid can be enhanced because of the specific cooperative coupling of water strong H-bond chain, connecting the carboxyl and amino groups (Panuszko et al. 2011), with the clathrate-like H-bond network surrounding the hydrocarbon side chain.

The correlations with the amino acid hydrophobicity indexes

Interesting observations appear from the correlation of the α parameter (Table 2) and the amino acid hydrophobicity values. Many authors have proposed different scales of hydrophobicity of amino acid side chains based on a variety of experimental and theoretical methods of measuring their hydrophobicity/electrophilicity specifity, such as solubility measurements or the free energy of transfer determinations. One of the most widely used scales has been proposed by Kyte and Doolittle (1982). This scale was derived from a combination of experimentally measured water–vapor transfer free energies for amino acids (Wolfenden et al. 1981) and the interior–exterior distribution of amino acid side-chains (Chothia 1976). The Kyte–Doolittle scale can be used for identifying both surface-exposed regions as well as transmembrane regions. Hessa et al. (2005) determined a biological hydrophobicity scale based on measurements of the apparent free energies of insertion for each amino acid residue to its position within the test segment. They found generally strong position dependence for polar and charged residues. Cornette et al. (1987) have reviewed the existing scales and developed a scale that is optimal for detecting amphipathic structures in proteins. Cid et al. (1992) proposed normalized hydrophobicity scale for alpha and beta proteins. There are fundamental differences between the suggested scales in ranking hydrophobicities of amino acids, as they measure different properties more or less directly related to hydrophobicity.

Values for selected hydrophobicity scales are shown in Table 2. The correlations between the contributions of vanishing weak hydrogen bonds (α parameter) and the amino acid hydrophobicity indexes from different scales are shown in Fig. 5. In the hydrophobicity scales, positive numbers are assigned to the amino acids with hydrophobic side chains and negative numbers to those with hydrophilic side chains.

From the data in Table 2 it can be seen that ranking hydrophobicities of the examined amino acids proposed by Kyte and Doolittle (1982) and Hessa et al. (2005) are in good agreement with the contributions of vanishing weak hydrogen bond sequences, except for proline. This disagreement is probably due to the fact that side chain of proline is connected twice with the backbone, thus restricting

its conformational flexibility. Additionally, proline, with respect to other amino acids, builds a ring including the amino group. We have found a good correlation for the contributions of vanishing weak hydrogen bonds and the Cid's hydrophobicity values (Cid et al. 1992) for the smaller amino acids, and slightly worse for larger amino acids. The opposite situation can be observed between α parameter and the hydrophobicity indexes proposed by Cornette et al. (1987).

Moreover, correlations between the α parameter and the amino acid hydrophobicity index (Cornette et al. 1987; Cid et al. 1992) (Fig. 5) show that the analyzed amino acids can be divided into two groups: the first group includes Gly, Ala and Pro, and the second one includes Ile, Val and Phe. Classification of amino acids into two groups based on the vanishing population of weak hydrogen bonds of water molecules is consistent with the division on the basis of the amino acid hydrophobicity indexes from different scales (Table 2). Independently, values of the most probable intermolecular oxygen–oxygen distance of water (R^{o}_{OO}) from Table 1 can already discriminate studied amino acids as belonging to the two discussed above groups.

Molecular dynamics results

Distance range of the first hydration sphere for each amino acid (Table 3) was determined from the radial distribution functions between the surface of amino acids and water molecules, as shown in "Supplementary Material".

The thickness of the first hydration sphere calculated from the MD data (Table 3) relative to the surface of Ile, Phe and Val is the same (0.47 nm) and is considerably greater than for Gly (0.35 nm) and Ala (0.36 nm), and to a lesser extent relative to Pro (0.44 nm). This observation indicates that the amino acids from the first group are hydrated in the similar way, which resembles hydrophobic hydration, where a solute molecule is closed in the cage of the water pseudo-clathrate structure. The amino acids from the second group reveal more hydrophilic hydration type, relying on direct hydrogen bond formation between water molecules and the amino acid polar groups. Such interpretation is also supported by the average numbers of hydrogen bonds between amino acids and hydration water shown in Table 3. These were calculated from MD trajectories using the standard geometric criterion, i.e., hydrogen bond is considered to exist if the distance A-D is less than 0.35 nm and the angle A-D-H is less than 40°, where A is the acceptor, D the donor and H is the proton (van der Spoel et al. 2010). It has to be added that the average number of hydrogen bonds obtained depends considerably on the angular cutoff used in the H-bond definition (see Fig. 9 in "Supplementary Material").

Comparison of the calculated average life time of hydrogen bonds between amino acids and hydration water (Table 3) is alike symptomatic in the discussed aspect. As expected, for all amino acids these hydrogen bonds persist on average 3–5 times longer than water–water hydrogen bonds in the bulk aqueous phase (2.15 ps). In the case of Ile, Val and Phe average life time of hydrogen bonds are longer than for smaller, more hydrophilic amino acids. It appears that for more hydrophobic amino acids, dynamics of water molecules H-bonded to polar groups is more restricted. It can result from the influence of relatively static and structured hydration sphere of the hydrocarbon side chain. In this context, it is worth noticing that the integral intensity of amino acid-affected HDO bands, shown in Table 1, decreases noticeably for larger, more hydrophobic solutes.

The integral intensity, measured as the area under the plot of the absorption coefficient against wavenumber, $\varepsilon(\nu)$, over the entire band, can change because of two reasons. The first one comes from a change of the derivative of the electric dipole moment in respect to vibration coordinate of the absorbing species, depending on the molecular surrounding and especially on the specific interaction, including hydrogen bond formation. It is well known that for water molecules involved in H-bond, the band of OH (OD) stretching vibration shifts linearly with its energy toward lower wavenumbers (the Badger–Bauer rule) accompanied by the approximately linear increase of the band integral intensity (Bergstrom et al. 1991; Glew and Rath 1971; Stangret and Gampe 1999). Inspection of values from Table 1, namely the band position (at the maximum or at the gravity centre) and the integral intensity of the OD band of HDO affected by amino acids, leads to a conclusion that

Table 3 Structural and dynamic properties of the hydration shell of amino acids obtained from molecular dynamics simulations

Amino acid	r^{a}	$\eta_{COO^-}{}^{b}$	$\eta_{NH3^+}{}^{b}$	$t_{COO^-}{}^{c}$	$t_{NH3^+}{}^{c}$
Gly	0.35	5.98	2.73	7.64	6.43
Ala	0.36	5.87	2.67	8.87	7.63
Pro	0.44	5.75	1.71	8.74	7.15
Val	0.47	5.76	2.64	10.37	9.75
Ile	0.47	5.75	2.63	10.61	9.95
Phe	0.47	5.79	2.64	9.83	9.52

[a] The thickness of the first hydration sphere calculated relative to the surface of the amino acids (nm)

[b] The average number of hydrogen bonds between the carboxyl (COO^-)/amino group (NH_3^+) and water

[c] The average life time of the hydrogen bonds between the carboxyl/amino group and water (ps). Hydrogen bond life times were determined by fitting a single exponential to the MD-derived H-bond autocorrelation function. Standard errors of hydrogen bonds are of the order of 0.3 %. Standard errors of average life time are of the order of 3 %

no simple relationship exists between these data. So, the difference observed in the integral intensity of the OD band of HDO affected by amino acids is determined by another factor. The second reason for variability of the intensity of the solute-affected water band can result from variability of the local density of water in the specific molecular arrangement around a solute. The integral intensity is independent of the concentration of the absorbing species in such a sense that it has been calculated using the average concentration of the species in the whole solution. Taking into account that considered species can form different local structures in solution, a different corresponding concentration can be expected. As a consequence, the vibrational band of the given local structure of the species can be characterized by the integral intensity value different from the mean value for the species in the whole solution. Thus, decreased integral band intensity of the solute-affected water can be explained by lower local concentration of water molecules hydrating hydrophobic side chain of amino acids, forming the ice-like open space structure. It should be noted that both reasons of the band intensity change discussed above are approximately independent: the first one depends on the energy of hydrogen bonding and the second one depends on the water geometrical structure.

The oxygen–oxygen distance distribution function of water molecules forming hydrogen bonds in the first hydration sphere of amino acids and for the bulk water has been also obtained on the basis of the MD simulation method. Unlike for infrared spectra, respective distance distribution function obtained from MD simulation can be calculated independently for water molecules directly H-bonded to amino acids (Fig. 6) as well as not directly associated (Fig. 7). Figure 6a compares the distribution function $P(R_{OO})$ for the bulk water obtained from the infrared spectra and from the MD simulation. As can be seen, the shapes of distribution functions differ: the distance distribution function from experimental data is narrower and its maximum is shifted towards longer distances. Such discrepancies have been reported previously (Panuszko et al. 2008, 2009). It should be emphasized that the mean distance obtained from both methods is practically the same (0.283 nm).

When comparing distance distribution functions obtained from the infrared spectra (Fig. 4) and from the MD (Figs. 6, 7) method one should keep in mind that the former depends on the two groups of water molecules: H-bonded to the solute as well as being under the influence of the solute in solution. On the basis of the differences between the distance distribution functions for water molecules directly H-bonded to the amino acids and the bulk water (Fig. 6b), it can be seen that these functions take small values and are very alike as all the solutes have the same centers of interactions (amino group and carboxyl group). The differences in intermolecular distance distribution obtained for water molecules not directly bonded to the solutes and for bulk water (Fig. 7b) can be divided into two groups: the first one corresponding to the small amino acids, like Pro, Gly and Ala, resembling the functions for water molecules directly H-bonded, and the second one corresponding to the larger amino acids (Ile, Val and Phe) possessing hydrophobic side chain, resembling the function for the bulk water. This result points to certain limitations of the conventional force-field based MD in describing hydrophobic solvation. This discrepancy can be ascribed to the fact that by construction non-polarizable force fields cannot properly describe the cooperativity of water hydrogen bond networks. The obtained result remains in general agreement with recent observations obtained from MD simulation (Galamba 2013): structural changes of water in

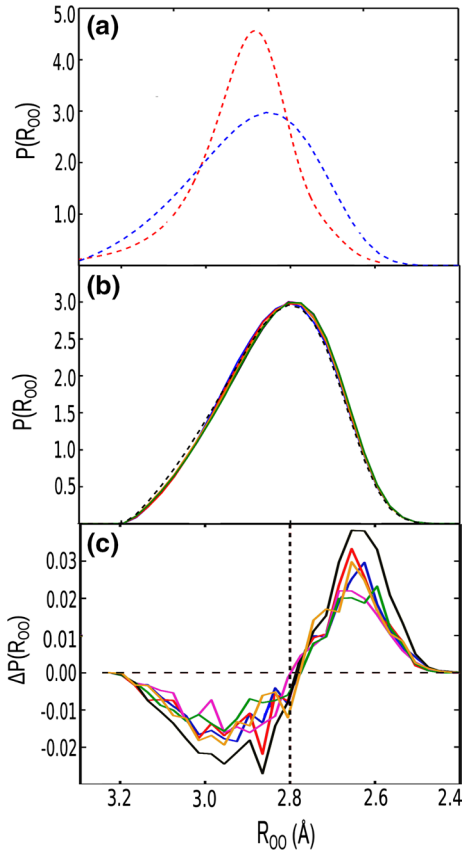

Fig. 6 **a** Comparison of the oxygen–oxygen distance distribution functions obtained from molecular dynamics (*blue*) and from the infrared spectral data (*red*) for bulk water. **b** Distance distribution functions for water molecules forming direct hydrogen bonds with the amino acids: Gly (*red*), Ala (*blue*), Pro (*black*), Val (*green*), Ile (*pink*) and Phe (*orange*). **c** Differences between the distance distribution functions for the water molecules forming direct hydrogen bonds with amino acids (panel **b**) and for bulk water (panel **a**): Gly (*red*), Ala (*blue*), Pro (*black*), Val (*green*), Ile (*pink*) and Phe (*orange*). The *vertical dashed line* shows the position of the most probable oxygen–oxygen distance for bulk water (color figure online)

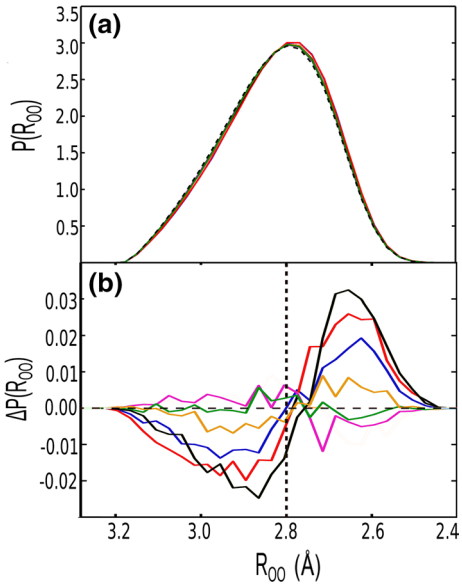

Fig. 7 **a** Distance distribution functions for water molecules in the hydration sphere of the amino acids, not involved in hydrogen bonds with the solute: Gly (*red*), Ala (*blue*), Pro (*black*), Val (*green*), Ile (*pink*) and Phe (*orange*). **b** Differences between the distance distribution functions for hydration water not involved in hydrogen bonds with the amino acids (panel **a**) and for the bulk water (panel **a** in Fig. 6): Gly (*red*), Ala (*blue*), Pro (*black*), Val (*green*), Ile (*pink*) and Phe (*orange*). The *vertical dashed line* shows the position of the most probable oxygen–oxygen distance for bulk water (color figure online)

the vicinity of small nonpolar solutes are unnoticeable from the water radial distribution functions; changes are only observed in a significantly enhanced tetrahedrality of water in the first hydration shell.

Conclusions

The effect of selected amino acids on the structure of the surrounding water has been studied by FTIR spectroscopy and by molecular dynamics simulations. The results of molecular dynamics helped to interpret spectral results. The agreement between received results is satisfactory and gives a consistent picture of the molecular details of the amino acid hydration in aqueous solution.

The obtained results show that the hydrogen bonds of water molecules around amino acids are stronger and shorter than those in pure water. The mean energy of water hydrogen bonds in the amino acid hydration sphere decrease in the following order: Ile > Val > Phe > Ala > Pro > Gly > bulk water. Both the experimental and theoretical results confirmed that the investigated amino acids can be divided into two groups: the first of them includes Val, Ile and Phe, and the second one contains small amino acids like Ala, Gly and Pro. Hydration of the amino acids from the first group is similar and resembles hydrophobic hydration, where a significant part of a solute molecule is closed in the cage of water pseudo-clathrate structure. The amino acids from the second group show more hydrophilic type of hydration, in which water molecules form direct hydrogen bonds with the amino acid centers of interaction. The vanishing contributions of weak hydrogen bonds of water molecules around amino acids decrease in the following order: Ile > Val > Phe > Ala > Pro > Gly and are in good agreement with ranking hydrophobicities of amino acid (Hessa et al. 2005; Kyte and Doolittle 1982).

Moreover, correlations between the vanishing population of weak hydrogen bonds of water molecules and the amino acid hydrophobicity indexes from different scales also show the division the analyzed amino acids into two groups mentioned before. Our analysis seems to point out that the hydrophobic side chain of amino acid exerts more pronounced hydration effect than normally expected for non-polar groups of other types of molecules. This can be realized by the specific cooperative coupling of the strong water H-bond chain between the carboxyl and the amino group of amino acid molecule (Panuszko et al. 2011) and the pseudo-clathrate network of water H-bonds including the hydrophobic side chain.

The most important aspect of this work is that, contrary to previous study results (Ide et al. 1997), we noticed differences in the hydration of analyzed amino acids and we pointed out their basis. These differences reflect the differences in the oxygen–oxygen distance distributions of water molecules, which result from various distributions of hydrogen bond energy between affected water molecules in the in the nearest surroundings of amino acids.

The detailed study of water structure around amino acids is essential for understanding the hydration process of larger systems, such as peptides and proteins and will help to better understand the influence of amino acids on the stability of proteins in aqueous solution.

Acknowledgments Thank are due to Dr. Piotr Bruździak for performance of chemometric analysis of FTIR spectra. This research was partially supported by the PL-Grid Infrastructure and TASK Computational Centre. This work was supported from the Republic of Poland scientific funds as a research project, within Grant No. 2013/11/B/NZ1/02258.

Conflict of interest The authors declare that they have no conflict of interest.

References

Anjum F, Rishi V, Ahmad F (2000) Compatibility of osmolytes with Gibbs energy of stabilization of proteins. BBA Protein Struct M 1476:75–84. doi:10.1016/s0167-4838(99)00215-0

Arakawa T, Timasheff SN (1985) The stabilization of proteins by osmolytes. Biophys J 47:411–414

Arakawa T, Tsumoto K, Kita Y, Chang B, Ejima D (2007) Biotechnology applications of amino acids in protein purification and formulations. Amino Acids 33:587–605. doi:10.1007/s00726-007-0506-3

Badger RM, Bauer SH (1937) Spectroscopic studies of the hydrogen bond. II. The shift of the O–H vibrational frequency in the formation of the hydrogen bond. J Chem Phys 5:839–851

Balabin RM (2010) The first step in glycine solvation: the glycine–water complex. J Phys Chem B 114:15075–15078. doi:10.1021/jp107539z

Bennion BJ, Daggett V (2004) Counteraction of urea-induced protein denaturation by trimethylamine N-oxide: a chemical chaperone at atomic resolution. Proc Natl Acad Sci USA 101:6433–6438. doi:10.1073/pnas.0308633101

Berendsen HJC, Postma JPM, Vangunsteren WF, Dinola A, Haak JR (1984) Molecular dynamics with coupling to an external bath. J Chem Phys 81:3684–3690. doi:10.1063/1.448118

Berglund B, Lindgren J, Tegenfeldt J (1978) O–H and O–D stretching vibrations in isotopically dilute hdo molecules in some solid hydrates. J Mol Struct 43:169–177. doi:10.1016/0022-2860(78)80004-0

Bergstrom PA, Lindgren J, Kristiansson O (1991) An IR study of the hydration of CLO4-, NO_3^-, Br^-, Cl^-, and SO_4^{2-} anions in aqueous solution. J Phys Chem 95:8575–8580. doi:10.1021/j100175a031

Bodor N, Gabanyi Z, Wong CK (1989) A new method for the estimation of partition coefficient. J Am Chem Soc 111:3783–3786. doi:10.1021/ja00193a003

Bolen DW, Baskakov IV (2001) The osmophobic effect: natural selection of a thermodynamic force in protein folding. J Mol Biol 310:955–963. doi:10.1006/jmbi.2001.4819

Bratos S, Leicknam JC, Pommeret S (2009) Relation between the OH stretching frequency and the OO distance in time-resolved infrared spectroscopy of hydrogen bonding. Chem Phys 359:53–57. doi:10.1016/j.chemphys.2009.03.016

Bruździak P, Panuszko A, Stangret J (2010) Chemometric determination of solute-affected solvent vibrational spectra as a superior way of information extraction on solute solvation phenomena. Vib Spectrosc 54:65–71. doi:10.1016/j.vibspec.2010.06.006

Bruździak P, Rakowska PW, Stangret J (2012) Chemometric method of spectra analysis leading to isolation of lysozyme and CtDNA spectra affected by osmolytes. Appl Spectrosc 66:1302–1310. doi:10.1366/11-06581

Bruździak P, Panuszko A, Stangret J (2013) Influence of osmolytes on protein and water structure: a step to understanding the mechanism of protein stabilization. J Phys Chem B 117:11502–11508

Burakowski A, Gliński J (2010) Hydration of amino acids from ultrasonic measurements. J Phys Chem B 114:12157–12161. doi:10.1021/jp105255b

Campo MG (2006) Molecular dynamics simulation of glycine zwitterion in aqueous solution. J Chem Phys 125:114511. doi:10.1063/1.2352756

Chaudhari A, Sahu PK, Lee SL (2004) Microsolvation effect on alanine: a many-body interaction study using ab initio method. Theochem J Mol Struc 683:115–119. doi:10.1016/j.theochem.2004.06.024

Chothia C (1976) Nature of accessible and buried surfaces in proteins. J Mol Biol 105:1–14. doi:10.1016/0022-2836(76)90191-1

Cid H, Bunster M, Canales M, Gazitua F (1992) Hydrophobicity and structural classes in proteins. Protein Eng 5:373–375. doi:10.1093/protein/5.5.373

Cornette JL, Cease KB, Margalit H, Spouge JL, Berzofsky JA, Delisi C (1987) Hydrophobicity scales and computational techniques for detecting amphipathic structures in proteins. J Mol Biol 195:659–685. doi:10.1016/0022-2836(87)90189-6

Daggett V (2006) Protein folding-simulation. Chem Rev 106:1898–1916. doi:10.1021/cr0404242

Darden T, York D, Pedersen L (1993) Particle mesh ewald: an N log(N) method for ewald sums in large systems. J Chem Phys 98:10089–10092. doi:10.1063/1.464397

Eriksson PO, Lindblom G, Burnell EE, Tiddy GJT (1988) Influence of organic solutes on the self-diffusion of water as studied by nuclear magnetic-resonance spectroscopy. J Chem Soc Faraday Trans I 84:3129–3139. doi:10.1039/f19888403129

Finney JL (1996) Hydration processes in biological and macromolecular systems. Faraday Discuss 103:1–18. doi:10.1039/fd9960300001

Finney JL, Soper AK (1994) Solvent structure and perturbations in solutions of chemical and biological importance. Chem Soc Rev 23:1–10. doi:10.1039/cs9942300001

Galamba N (2013) Water's Structure around hydrophobic solutes and the iceberg model. J Phys Chem B 117:2153–2159. doi:10.1021/jp310649n

Gavezzotti A (1983) The calculation of molecular volumes and the use of volume analysis in the investigation of structured media and of solid-state organic-reactivity. J Am Chem Soc 105:5220–5225. doi:10.1021/ja00354a007

Glew DN, Rath NS (1971) H_2O, HDO, and CH_3OH infrared spectra and correlation with solvent basicity and hydrogen bonding. Can J Chem 49:837. doi:10.1139/v71-142

Gojlo E, Śmiechowski M, Stangret J (2005) The common effect of hydrophobic and electrophilic types of hydration dependent on protonation in the sec-butylamine/HCl/H_2O system studied by FTIR spectroscopy. J Mol Struct 744:809–814. doi:10.1016/j.molstruc.2004.11.005

Gojlo E, Gampe T, Krakowiak J, Stangret J (2007) Hydration of aprotic donor solvents studied by means of FTIR spectroscopy. J Phys Chem A 111:1827–1834. doi:10.1021/jp065599p

Gojlo E, Śmiechowski M, Panuszko A, Stangret J (2009) Hydration of carboxylate anions: infrared spectroscopy of aqueous solutions. J Phys Chem B 113:8128–8136. doi:10.1021/jp811346x

Head-Gordon T (1995) Is water structure around hydrophobic groups clathrate-like? Proc Natl Acad Sci USA 92:8308–8312. doi:10.1073/pnas.92.18.8308

Hecht D, Tadesse L, Walters L (1993) Correlating hydration shell structure with amino acid hydrophobicity. J Am Chem Soc 115:3336–3337. doi:10.1021/ja00061a045

Hernandez B, Pfluger F, Nsangou M, Ghomi M (2009) Vibrational analysis of amino acids and short peptides in hydrated media. IV. Amino acids with hydrophobic side chains: L-Alanine, L-Valine, and L-Isoleucine. J Phys Chem B 113:3169–3178. doi:10.1021/jp809204d

Hess B, Kutzner C, van der Spoel D, Lindahl E (2008) GROMACS 4: algorithms for highly efficient, load-balanced, and scalable molecular simulation. J Chem Theory Comput 4:435–447. doi:10.1021/ct700301q

Hessa T, Kim H, Bihlmaier K, Lundin C, Boekel J, Andersson H, Nilsson I, White SH, von Heijne G (2005) Recognition of transmembrane helices by the endoplasmic reticulum translocon. Nature 433:377–381. doi:10.1038/nature03216

Ide M, Maeda Y, Kitano H (1997) Effect of hydrophobicity of amino acids on the structure of water. J Phys Chem B 101:7022–7026. doi:10.1021/jp971334m

Jamal S, Poddar NK, Singh LR, Dar TA, Rishi V, Ahmad F (2009) Relationship between functional activity and protein stability in the presence of all classes of stabilizing osmolytes. FEBS J 276:6024–6032. doi:10.1111/j.1742-4658.2009.07317.x

Kumar S, Rai AK, Singh VB, Rai SB (2005) Vibrational spectrum of glycine molecule. Spectrochim Acta 61:2741–2746. doi:10.1016/j.saa.2004.09.029

Kumar R, Schmidt JR, Skinner JL (2007) Hydrogen bonding definitions and dynamics in liquid water. J Chem Phys 126:204107. doi:10.1063/1.2742385

Kyte J, Doolittle RF (1982) A simple method for displaying the hydropathic character of a protein. J Mol Biol 157:105–132. doi:10.1016/0022-2836(82)90515-0

Liu YF, Bolen DW (1995) The peptide backbone plays a dominant role in protein stabilization by naturally-occurring osmolytes. Biochemistry 34:12884–12891. doi:10.1021/bi00039a051

McLain SE, Soper AK, Terry AE, Watts A (2007) Structure and hydration of L-proline in aqueous solutions. J Phys Chem B 111:4568–4580. doi:10.1021/jp068340f

McMullan R, Jeffrey GA (1959) Hydrates of the tetra N-butyl and tetra I-amyl quaternary ammonium salts. J Chem Phys 31:1231–1234. doi:10.1063/1.1730574

McMullan RK, Bonamico M, Jeffrey GA (1963) Polyhedral clathrate hydrates. V. Structure of tetra-*N*-butyl ammonium fluoride hydrate. J Chem Phys 39:3295–3310. doi:10.1063/1.1734193

Michaux C, Wouters J, Perpete EA, Jacquemin D (2009) Ab initio investigation of the hydration of deprotonated amino acids. J Am Soc Mass Spectr 20:632–638. doi:10.1016/j.jasms.2008.11.025

Mullin JM, Gordon MS (2009) Alanine: then there was water. J Phys Chem B 113:8657–8669. doi:10.1021/jp901459y

Niehues G, Heyden M, Schmidt DA, Havenith M (2011) Exploring hydrophobicity by THz absorption spectroscopy of solvated amino acids. Faraday Discuss 150:193–207. doi:10.1039/c0fd00007h

Olsztynska S, Komorowska M, Vrielynck L, Dupuy N (2001) Vibrational spectroscopic study of L-phenylalanine: effect of pH. Appl Spectrosc 55:901–907. doi:10.1366/0003702011952703

Oostenbrink C, Soares TA, van der Vegt NFA, van Gunsteren WF (2005) Validation of the 53A6 GROMOS force field. Eur Biophys J Biophy 34:273–284. doi:10.1007/s00249-004-0448-6

Pacios LF (2001) Distinct molecular surfaces and hydrophobicity of amino acid residues in proteins. J Chem Inf Comp Sci 41:1427–1435. doi:10.1021/ci010369n

Panuszko A, Gojlo E, Zielkiewicz J, Śmiechowski M, Krakowiak J, Stangret J (2008) Hydration of simple amides. FTIR spectra of HDO and theoretical studies. J Phys Chem B 112:2483–2493. doi:10.1021/jp7099509

Panuszko A, Bruździak P, Zielkiewicz J, Wyrzykowski D, Stangret J (2009) Effects of urea and trimethylamine-*N*-oxide on the properties of water and the secondary structure of hen egg white lysozyme. J Phys Chem B 113:14797–14809. doi:10.1021/jp904001m

Panuszko A, Śmiechowski M, Stangret J (2011) Fourier transform infrared spectroscopic and theoretical study of water interactions with glycine and its *N*-methylated derivatives. J Chem Phys 134:115104. doi:10.1063/1.3567202

Panuszko A, Wojciechowski M, Bruździak P, Rakowska PW, Stangret J (2012) Characteristics of hydration water around hen egg lysozyme as the protein model in aqueous solution. FTIR spectroscopy and molecular dynamics simulation. Phys Chem Chem Phys 14:15765–15773. doi:10.1039/c2cp42229h

Pieniazek PA, Stangret J (2005) Hydration of tetraethylammonium tetrafluoroborate derived from FTIR spectroscopy. Vib Spectrosc 39:81–87. doi:10.1016/j.vibspec.2004.11.004

Praprotnik M, Janezic D, Mavri J (2004) Temperature dependence of water vibrational spectrum: a molecular dynamics simulation study. J Phys Chem A 108:11056–11062. doi:10.1021/jp046158d

Shiraki K, Kudou M, Fujiwara S, Imanaka T, Takagi M (2002) Biophysical effect of amino acids on the prevention of protein aggregation. J Biochem 132:591–595

Shirts MR, Pande VS (2005) Solvation free energies of amino acid side chain analogs for common molecular mechanics water models. J Chem Phys 122:134508. doi:10.1063/1.1877132

Śmiechowski M, Stangret J (2007) Molecular picture of hydroxide anion hydration in aqueous solutions studied by FT-IR ATR spectroscopy. J Mol Struct 834:239–248. doi:10.1016/j.molstruc.2006.09.040

Śmiechowski M, Stangret J (2008) ATR FT-IR H2O spectra of acidic aqueous solutions. Insights about proton hydration. J Mol Struct 878:104–115. doi:10.1016/j.molstruc.2007.08.001

Śmiechowski M, Stangret J (2010) Vibrational spectroscopy of semi-heavy water (HDO) as a probe of solute hydration. Pure Appl Chem 82:1869–1887. doi:10.1351/pac-con-09-10-14

Soper AK, Castner EW, Luzar A (2003) Impact of urea on water structure: a clue to its properties as a denaturant? Biophys Chem 105:649–666. doi:10.1016/s0301-4622(03)00095-4

Stangret J (1988) Solute-affected vibrational-spectra of water in $Ca(ClO_4)_2$ aqueous-solutions. Spectrosc Lett 21:369–381. doi:10.1080/00387018808082314

Stangret J, Gampe T (1999) Hydration sphere of tetrabutylammonium cation. FTIR studies of HDO spectra. J Phys Chem B 103:3778–3783. doi:10.1021/jp983199z

Stangret J, Gampe T (2005) Hydration of tetrahydrofuran derived from FTIR spectroscopy. J Mol Struct 734:183–190. doi:10.1016/j.molstruc.2004.09.021

Sun J, Niehues G, Forbert H, Decka D, Schwaab G, Marx D, Havenith M (2014) Understanding thz spectra of aqueous solutions: glycine in light and heavy water. J Am Chem Soc 136:5031–5038. doi:10.1021/ja4129857

Taneja S, Ahmad F (1994) Increased thermal-stability of proteins in the presence of amino acids. Biochem J 303:147–153

Timasheff SN (2002) Protein-solvent preferential interactions, protein hydration, and the modulation of biochemical reactions by solvent components. Proc Natl Acad Sci USA 99:9721–9726. doi:10.1073/pnas.122225399

Troitzsch RZ, Martyna GJ, McLain SE, Soper AK, Crain J (2007) Structure of aqueous proline via parallel tempering molecular dynamics and neutron diffraction. J Phys Chem B 111:8210–8222. doi:10.1021/jp0714973

Turner J, Soper AK (1994) The effect of apolar solutes on water-structure—alcohols and tetraalkylammonium ions. J Chem Phys 101:6116–6125. doi:10.1063/1.467327

van der Spoel D, Lindahl E, Hess B, van Buuren AR, Apol E, Meulenhoff PJ, Tieleman DP, Sijbers ALTM, Feenstra KA, van Drunen R et al. (2010) Gromacs User Manual version 4.5.4, www.gromacs.org

Wang AJ, Bolen DW (1996) Effect of proline on lactate dehydrogenase activity: testing the generality and scope of the compatibility paradigm. Biophys J 71:2117–2122

Wang AJ, Bolen DW (1997) A naturally occurring protective system in urea-rich cells: mechanism of osmolyte protection of proteins against urea denaturation. Biochemistry 36:9101–9108. doi:10.1021/bi970247h

Wolfenden R, Andersson L, Cullis PM, Southgate CCB (1981) Affinities of amino-acid side-chains for solvent water. Biochemistry 20:849–855. doi:10.1021/bi00507a030

Yancey PH, Clark ME, Hand SC, Bowlus RD, Somero GN (1982) Living with water-stress—evolution of osmolyte systems. Science 217:1214–1222. doi:10.1126/science.7112124

Zhu GY, Zhu X, Fan Q, Wan XL (2011) Raman spectra of amino acids and their aqueous solutions. Spectrochim Acta A 78:1187–1195. doi:10.1016/j.saa.2010.12.079